

Investigation of Magnetic Anisotropy and Heat Dissipation in Thin Films of Compensated Antiferromagnet CuMnAs by Pump-probe Experiment

M. Surýnek¹, V. Saidl¹, V. Novák², R.P. Campion³, P. Wadley³, and P. Němec^{1,*}

¹*Faculty of Mathematics and Physics, Charles University, Ke Karlovu 3, 121 16 Prague 2, Czech Republic*

²*Institute of Physics ASCR, v.v.i., Cukrovarnická 10, 162 53 Prague 6, Czech Republic*

³*School of Physics and Astronomy, University of Nottingham, Nottingham NG7 2RD, United Kingdom*

Recently, the possibility to determine the easy axis position in 10 nm thick film of compensated antiferromagnet CuMnAs with in-plane uniaxial magnetic anisotropy by magneto-optical pump and probe experiment was reported [Nature Photonics 11, 91 (2017)]. In this contribution we discuss the applicability of this method for the investigation of a broader set of epitaxial CuMnAs films having different thicknesses. It was revealed that the in-plane magnetic anisotropy can be studied only in samples where this anisotropy is rather strong. On the other hand, in samples with a weak magnetic anisotropy the impact of a strong pump pulse itself induces considerable anisotropy changes and, therefore, the magnetic anisotropy measured by the pump-probe technique differs substantially from that in the equilibrium conditions. However, the major achievement reported in this paper is that optical pump-probe experiment can be used very efficiently to study the local heating and heat dissipation in CuMnAs epitaxial layers. In particular, it was revealed that for a local film heating by a focused laser the thinner films are heated more but the heat is dissipated considerably faster than in the case of thicker films. This illustrates that optical pump-probe experiment is a valuable characterization tool for the heat management optimization in the CuMnAs memory devices and can be applied in a similar way as was used previously during the heat-assisted magnetic recording (HAMR) technology development for a latest generation of hard drive discs.

I. INTRODUCTION

Antiferromagnets (AFs) are very promising materials for spintronic applications thanks to many interesting properties they combine [1-4]. For instance, the absence of net magnetization and stray fields eliminates crosstalk between neighboring devices that enables

* Electronic mail: nemec@karlov.mff.cuni.cz

their high-density arrangement and makes them robust against external magnetic fields. Moreover, due to the presence of a strong exchange coupling between the sublattices in AFs, the intrinsic resonance frequencies are in the terahertz frequency range, in contrast to gigahertz frequencies in ferromagnets (FMs), which offers a prospect of an extremely fast operation of the devices [5]. On the other hand, the absence of a net magnetic moment, the frequently observed small size of magnetic domains and the ultrafast magnetization dynamics make probing of antiferromagnetic order by common magnetometers or magnetic resonance techniques notoriously difficult. Therefore, the possibility to study AFs by optical techniques attracts a significant attention nowadays [6]. Moreover, optics can be used not only to study AFs passively, but also to actively manipulate its magnetic order [7,8]. Recent breakthroughs in electrical detection and manipulation of antiferromagnets have opened a new avenue in the research of non-volatile spintronic devices. The first experimental realization of all-electrical room-temperature USB-compatible antiferromagnetic memory chips was reported in antiferromagnetic metal CuMnAs [9]. In this material also an ultrafast writing in the memory device by the irradiation with a single THz pulse was demonstrated [10]. Recently, we have developed an experimental technique allowing us to determine the easy axis position in 10 nm thick film of compensated antiferromagnet CuMnAs with in-plane uniaxial magnetic anisotropy by magneto-optical pump and probe experiment [11]. In this contribution we discuss the applicability of this method for the investigation of a broader set of epitaxial MBE-grown CuMnAs samples having different thicknesses. Moreover, we demonstrate that optical pump-probe signals can be very efficiently used to study the local heating and heat dissipation in CuMnAs films.

II. EXPERIMENTAL TECHNIQUE AND SAMPLES

We employed the pump-probe technique of ultrafast laser spectroscopy. As the light source was used a tunable femtosecond Ti:Sapphire oscillator (Mai Tai, Spectra Physics) that is producing laser pulses with time-width of 150 fs with a repetition rate of 80 MHz. In a standard (degenerate) pump-probe experiments, the laser output was divided into strong pump pulses with a fluence of $\approx 3 \text{ mJ cm}^{-2}$ and probe pulses with at least 50 times weaker fluence. For the non-degenerate pump-probe experiment, when pump and probe pulses have different wavelengths, the optical parametric oscillator (Inspire, Spectra Physics) was used as a source of probe pulses and depleted fundamental beam was used as the pump beam. Time delay between pump and probe pulses was controlled by computer-controlled delay line in pump

beam. Typically, experiments were performed in nearly normal incidence geometry with an angle between pump and probe beam of 6° when pump and probe pulses were focused to a same spot on the sample with a spot-size of $\approx 30 \mu\text{m}$ (full width at half maximum, FWHM). Control experiments were performed also with collinearly propagating pump and probe pulses that were focused by a microscopic objective to a laser spot-size of $\approx 1.5 \mu\text{m}$ [12]. The samples were mounted in a closed-cycle helium cryostat (ARS) and the experiments were performed at base temperature of 15 K. Probe pulses transmitted and reflected from the sample were led to the detection parts of the setup. Here the difference and sum of signals from detectors were measured by the optical bridge [13]. The difference signal is proportional to the magneto-optical (MO) signal corresponding to the probe polarization rotation. The sum signal corresponds to the differential reflectivity dR/R and the differential transmission dT/T for reflected and transmitted probe pulses, respectively. If the changes in transmission are small, the differential transmission $dT/T \sim \Delta\alpha d$, where d is the sample thickness and $\Delta\alpha$ is the pump-induced change of the absorption coefficient [14].

In this study we investigated a fully compensated collinear antiferromagnetic semimetal CuMnAs. A broad set of CuMnAs thin epitaxial films, with layer thicknesses varying from 8 to 60 nm, were grown on GaP(100) substrate by molecular beam epitaxy both in Prague (Institute of Physics, Academy of Sciences of the Czech Republic) and Nottingham (School of Physics and Astronomy, University of Nottingham). To prevent the oxidation of CuMnAs surface, a protective ≈ 2 nm Al cap was grown on each CuMnAs epilayer. Magnetic moments are lying in-plane of CuMnAs films and its tetragonal lattice is matched to GaP(100) by 45° rotation (CuMnAs{100} is parallel to GaP{110}) [15]. Previous detailed studies of magnetic anisotropy of CuMnAs films by X-ray magnetic linear dichroism (XMLD) spectroscopy revealed that films with a thickness of about 10 nm have uniaxial magnetic anisotropy along the [110] crystallographic direction of the GaP substrate [11,16], which corresponds to the [100] direction in CuMnAs. On the other hand, thicker films show biaxial magnetic anisotropy along the [100] and [010] directions in CuMnAs [17,18].

III. RESULTS AND DISCUSSION

A. TIME RESOLVED MAGNETO-OPTICAL EXPERIMENT

In fully compensated collinear antiferromagnet CuMnAs, the signals from oppositely oriented magnetic sublattices cancel in equilibrium for MO effects which are linear in magnetization (i.e., Kerr effect and Faraday effect). Hence, only MO effects which are quadratic

(even) in magnetization can be used to investigate properties of this material by MO means [6]. Voigt effect is a quadratic MO effect that leads to a rotation of the polarization plane of linearly polarized light (or change of its ellipticity) when the magnetic moments are perpendicular to the light propagation direction. Phenomenologically, this effect can be described by a different complex index of refraction for light with a polarization plane oriented parallel and perpendicular to the magnetic moments, respectively [19,20]. The polarization rotation due to Voigt effect is typically rather small in comparison with other (non-magnetic) sources of light polarization changes [8,21,22]. In order to separate the actual MO signal from non-magnetic contributions to the total polarization rotation experienced by light in the investigated sample, we utilized pump-probe technique [11], as schematically depicted in Fig. 1a. The pump-induced local heating of the sample leads to its partial demagnetization [23,24] and, consequently, to a reduction of the MO signal. The measured dynamical MO signal in pump-probe experiment is given by [11]

$$MO(\Delta t, \epsilon) = \frac{2P}{M} \sin 2(\varphi - \epsilon) \delta M(\Delta t) + D \quad (1)$$

where P corresponds to MO coefficient of Voigt effect, which is scaling quadratically with the sublattice magnetization M projection onto the plane perpendicular to the probe light propagation direction, and φ and ϵ describe the in-plane orientation of magnetic moments and light polarization, respectively. δM is a pump-induced change of magnetization, which depends on time delay Δt between pump and probe pulses, and D is a polarization-insensitive background, which is coming mainly from the substrate.

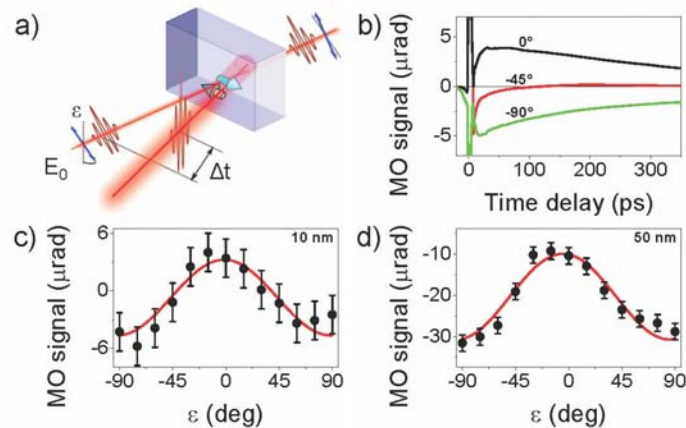


Figure 1: Pump-probe magneto-optical experiment in CuMnAs. (a) Schematic illustration of the pump-induced reduction of Voigt effect MO signal that is measured for various incident probe polarization orientations ϵ as a function of time delay Δt between pump and probe pulses. (b) Time-resolved MO data measured in transmission geometry in 10 nm thick film grown in Prague using pump and probe pulses with wavelength of 820 nm. (c) Polarization dependence of MO signal at $\Delta t = 60$ ps for the same sample as in (b); polarization orientation $\epsilon = -45^\circ$ corresponds to the crystallographic direction [110] in the GaP substrate. (d) Same dependence as in (c) for 50 nm thick film grown in Prague.

As a typical example, we show in Fig. 1b the time-resolved dynamics of pump-induced change of MO signal in 10 nm thick epilayer of CuMnAs in transmission geometry for 3 selected orientations of incident light polarization plane ε . At time delay $\Delta t = 0$ ps the strong pump pulse locally heats the sample (approximately by 100 K, see Fig. 4 in Ref. 11) causing its partial demagnetization. Consequently, the probe pulses measure the pump-induced polarization rotation change with a characteristic harmonic dependence on ε , which is described by Eq. (1). A detailed polarization dependence of MO signal at time delay $\Delta t = 60$ ps is shown in Fig. 1c. As expected [11], the deduced polarization dependence for this 10 nm epilayer has symmetry corresponding to an uniaxial sample with an easy axis located along one of the polarization orientations where the measured MO signal is "zero" (i.e., for $\varepsilon = \pm 45^\circ$ in this case). If needed, this ambiguity of the Néel vector orientation determination can be removed by an additional experiment when the sample tilting around these two directions is performed (see Fig. 2 in Ref. 11). The situation for thicker films, which have biaxial magnetic anisotropy, is more complicated. If magnetic domains were larger than the laser spot-size and the laser spot were located within a single magnetic domain, all the magnetic moments sensed by the laser would be pointing along the same direction and the detected MO signal would have again the symmetry predicted by Eq. (1). Consequently, in two domains having moments rotated by 90° the MO signals would have opposite sign. However, as the domain size of biaxial CuMnAs films does not exceed a few micrometers [17,18], which is considerably less than the laser spot-size of $\approx 30 \mu\text{m}$ in this experiment, several domains should be sampled simultaneously by the laser beam and, consequently, the detected MO signals should average out to zero. In reality, this is not what we observed experimentally as demonstrated by Fig. 1d where MO data measured in 50 nm epilayer are shown. Overall, very similar results, both from the symmetry point of view and also with respect to the magnitude of detected MO signals, were obtained in all the studied samples (with a thickness from 8 to 60 nm) and for two different spot-sizes (30 and $1.5 \mu\text{m}$) for many different positions on the samples.

In the following, we discuss the origin of this discrepancy between the results obtained by XMLD, where a change of CuMnAs magnetic anisotropy from uniaxial [11,16] to biaxial [17,18] was observed when the epilayer thickness was increased from ≈ 10 to 50 nm, respectively, and our pump-probe experiments, where very similar results were obtained for all the investigated samples with thicknesses varying from 8 to 60 nm. One possible explanation of this difference might be a different depth sensitivity of these two techniques. The XMLD experiment was performed in a reflection geometry using a total electron yield that leads to a

probing depth of ≈ 3 nm, which is smaller than the typical CuMnAs film thickness. On the other hand, the optical pump–probe experiment is performed in transmission geometry where the whole material is probed with the same sensitivity. However, considerably more probable is another explanation: XMLD seems to detect the actual magnetic anisotropy of the CuMnAs epilayers in experimental conditions close to the thermodynamic equilibrium. On the contrary, the inherent part of the pump–probe technique is a local transient heating of the sample by a pump pulse with a typical temperature increase of ≈ 100 K [11]. The in-plane magnetic anisotropy in CuMnAs films is apparently rather weak and, therefore, this temperature increase seems to lead to a considerable reduction of the material magnetic anisotropy and/or nano-fragmentation of the domains within the irradiated spot, as schematically depicted in Fig. 2, where the MO signal due to the volume of the CuMnAs film is averaged out to zero. The remaining uniaxial magnetic anisotropy, which we observed in all the studied samples (see Figs. 1c and 1d), is probably the (relatively strong) uniaxial magnetic anisotropy induced in the interfacial layer of CuMnAs that comes from the specific symmetry of bond alignments on the CuMnAs/GaP interface [11]. This explanation is also fully in accord with our previous observation that in the Fe/CuMnAs bilayer we did not observe in the pump-probe experiment, unlike in XMLD experiment, any significant reorientation of magnetic moments in CuMnAs by external magnetic field due to the interlayer exchange coupling with Fe [25]. Moreover, the nano-fragmentation of magnetic domains due to the film local heating was suggested as an origin of the large electrical readout signals measured in CuMnAs memory devices after strong electrical and optical writing very recently [26].

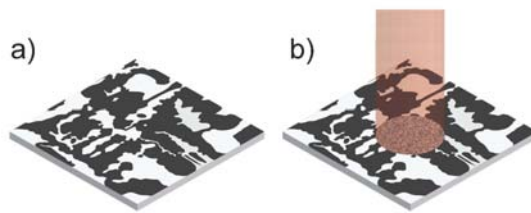


Figure 2: Schematic illustration of the magnetic domain structure change due to pump-induced heating of the sample. (a) Equilibrium domain structure. (b) Local change of the domain structure due to the laser.

B. TRANSIENT REFLECTIVITY AND ABSORPTION

In the previous section we have shown that pump-probe *magneto-optical* experiments do not provide information about the magnetic anisotropy in CuMnAs films in equilibrium. In this section we demonstrate that pump-probe *optical* experiments can be used very efficiently to study dynamics of heating and heat dissipation in these films.

The photoexcitation of a metal by an intense femtosecond laser pulse excites the electron distribution out of equilibrium on a time scale much shorter than the electron-phonon interaction time. The resulting non-thermal population of electrons thermalizes rapidly by electron-electron scattering processes. Consequently, a thermalized electron system, which can be described by a Fermi distribution with an electron temperature T_e , is formed within ≈ 100 fs after the impact of pump pulse [27-29]. On a picosecond timescale, the excess energy is dissipated from the electron system to the lattice by electron-phonon scattering processes, which leads to an increase of the lattice temperature T_{lat} . Finally, the heat diffusion and generation of coherent stress waves dissipates the excess energy and the metal returns to the equilibrium state. Importantly, all the above effects lead to a change of optical properties and, therefore, the corresponding characteristic time constants can be evaluated from the measured optical transients [27-29]. Experimentally, this is usually achieved by a degenerate pump-probe experiment where a time evolution of differential reflectivity dR/R is measured by probe pulses of the same wavelength (λ) as that of the pump pulse [28]. The measured reflectivity dynamics can be reproduced by a phenomenological equation [29]

$$\Delta R/R(\Delta t, \lambda) = [\alpha(\lambda)(1 - e^{-\Delta t/\tau_{ee}})e^{-\Delta t/\tau_{ep}} + \beta(\lambda)(1 - e^{-\Delta t/\tau_{ep}})]e^{-\Delta t/\tau_{th}}. \quad (2)$$

The first term, with a spectral weight α , represents the electronic response with a rise time described by the electron-electron thermalization time τ_{ee} and decaying by an energy transfer to the lattice with the characteristic electron-phonon relaxation time τ_{ep} . The second term, with a spectral weight β , describes the lattice heating, with the same time constant time τ_{ep} , and the thermal relaxation time τ_{th} represents the heat diffusion outside the irradiated area. The heat capacity of the electron system is much smaller than the heat capacity of the lattice. Consequently, for $\Delta t \gg \tau_{ep}$, when $T_e = T_{lat}$, almost all the excess energy is stored in the lattice system and the contribution from the electron system to the measured change of optical properties is negligible [27-29]. In general, a detailed interpretation of the differential reflectivity can be very complex because the magnitude and even sign of α and β depend strongly on details of the electronic band structure and wavelength of probe pulses [27-29] (see also Fig. 3). Consequently, for an unambiguous separation of individual contributions to the measured signals, it is very advantageous to measure the differential reflectivity at several probe wavelengths [27,29] and/or to supplement it with measurements of the differential transmission dT/T [27].

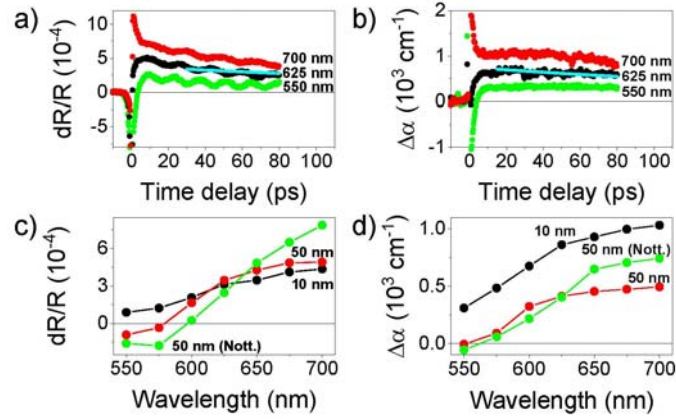


Figure 3: (a) and (b) Time-resolved dynamics of differential reflectivity dR/R (a) and absorption coefficient change $\Delta\alpha$ (b) measured in 10 nm thick film grown in Prague for 3 selected wavelengths of probe pulses after excitation by pump pulses at 820 nm (points). Lines are monoexponential decay fits. (c) and (d) Spectral dependence of dR/R (c) and $\Delta\alpha$ (d) at $\Delta t = 60$ ps (i.e., signals coming from the lattice) for 10 nm and 50 nm films grown in Prague and for 50 nm film grown in Nottingham.

In Fig. 3a and Fig. 3b we show the dynamics of differential reflectivity dR/R and pump-induced change of absorption coefficient $\Delta\alpha$, respectively, that was measured by probe pulses of several wavelengths in 10 nm film prepared in Prague. The strong wavelength dependence of the initial dynamics (the sign change, in particular) clearly identifies the contribution coming from the electron system. Consequently, it shows that the temperature of electrons and lattice is equilibrated after $\Delta t \approx 10$ ps (where this strongly wavelength dependent signal from the electron system is absent). Rather similar results were obtained also for films with other thicknesses. For example, the spectral dependence of optical signals coming from the lattice (see Fig. 3c and Fig. 3d) is monotonous in the investigated spectral range and it seems to be spectrally shifted towards longer wavelengths in thicker films. The measured data also reveal the very similar optical (and thermal, see Fig. 4b and 4c) properties of CuMnAs films grown in Prague and Nottingham and, therefore, points to a high reproducibility of the film growth process. However, the most important conclusion within the context of this paper is that it is possible to determine the dynamics of heat dissipation from the measured data, which corresponds to the monoexponential decay fits of the measured dynamics for long time delays [cf. Eq. (2)]. Interestingly, the fitting procedure is easier to perform in the measured dynamics of $\Delta\alpha$ than in dR/R where the thermal relaxation-related signal dominates after longer time delays (see Figs. 3a and 3b). Moreover, the fitting of dR/R is also complicated by the presence of an oscillatory signal that is due to the propagation of coherent stress waves in the GaP substrate (see Figs. S9 and S10 and the adjacent discussion in the Supplementary information of Ref. 11). The heat dissipation dynamics in films of different thicknesses is compared in

Fig. 4. The measured data clearly show that the heat is dissipated faster in thinner films – see Fig. 4c. Moreover, assuming that the change of optical constants is linear in the lattice temperature [28], our data indicate that the pump-induced local heating of the lattice is larger in thinner films – see Fig. 4b.

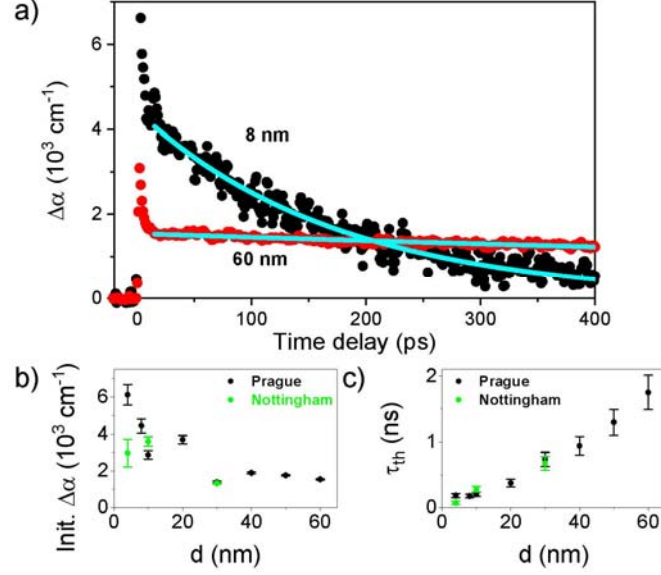


Figure 4: Local heating and heat dissipation in CuMnAs films of different thicknesses. (a) Dynamics of $\Delta\alpha$ measured for 8 nm and 60 nm films grown in Prague by pump and probe pulses with wavelength of 820 nm (points); lines depict the monoexponential decay fits revealing the thermal relaxation time τ_{th} . (b) and (c) Dependence of initial value of $\Delta\alpha$ (b) and thermal relaxation time τ_{th} (c) on epilayer thickness for samples grown in Prague and Nottingham.

IV. CONCLUSIONS

In this contribution we discussed the research potential of pump-probe experiment for the investigation of a compensated metal antiferromagnet CuMnAs. We revealed that the previously demonstrated technique for studying magnetic anisotropy, which is based on measurement of magneto-optical pump-probe signals (Ref. 11), is applicable only for samples where the uniaxial magnetic anisotropy is rather strong. In samples with a weak magnetic anisotropy, which seems to be the case for a vast majority of CuMnAs epitaxial layers, the impact of a strong pump pulse itself induces considerable changes of the magnetic anisotropy and, therefore, the magnetic anisotropy measured by the pump-probe technique differs substantially from that in the equilibrium conditions. Nevertheless, the assumed pump-induced nano-fragmentation of magnetic domains can be closely connected with the recently observed large electrical readout signals measured in CuMnAs memory devices when strong electrical and optical writing is performed (Ref. 26). However, the major achievement reported in this

paper is that optical pump-probe signals can be very efficiently used to study the heating and heat dissipation in CuMnAs films. In particular, we revealed that for local film heating, by the femtosecond laser with a spot-size of $\approx 30 \mu\text{m}$, the thinner films are heated more but the heat is dissipated considerably faster than in the case of thicker films. This optical pump-probe experiment could be, therefore, used very efficiently as a characterization tool for the heat management optimization in the CuMnAs memory devices in a similar way that it was applied during the heat-assisted magnetic recording (HAMR) technology development for the recent generation of the hard drive discs (HDDs) [30]. In particular, in HDDs the pump-probe studies enabled to achieve an extremely fast cooling of the recorded bits due to an efficient vertical heat diffusion using an optimized heat sink underlayer structure (see Fig. 18 in Ref. 30). The experimentally observed large electrical readout signals in CuMnAs memory devices after application of strong electrical and optical writing pulses are connected with a local heating of the CuMnAs films [26]. Therefore, a detailed spatially- and time-resolved optical pump-probe study of heat dissipation in CuMnAs films and the role of a substrate in this process, for example, can be extremely important for the future development of memory devices from this material.

ACKNOWLEDGMENTS

This work was supported in part by the Grant Agency of the Czech Republic under EXPRO grant no. 19-28375X, by EU FET Open RIA under grant no. 766566, from the Charles University grants no. 1582417 and no. SVV-2019-260445, the Engineering and Physical Sciences Research Council under grant no. EP/P019749/1, and by the Ministry of Education of the Czech Republic Grant LM2018110. P.W. acknowledges support from the Royal Society through a University Research Fellowship.

AVAILABILITY OF DATA

The data that support the findings of this study are available from the corresponding author upon reasonable request.

REFERENCES

- [1] T. Jungwirth, X. Marti, P. Wadley, and J. Wunderlich, *Nature Nanotechnology* **11**, 231 (2016).
- [2] V. Baltz, A. Manchon, M. Tsoi, T. Moriyama, T. Ono, and Y. Tserkovnyak, *Rev. Mod. Phys.* **90**, 015005 (2018).
- [3] R.A. Duine, K.-J. Lee, S.S.P. Parkin, and M.D. Stiles, *Nature Physics* **14**, 217 (2018).
- [4] E.V. Gomonay and V.M. Loktev, *Low Temperature Physics* **40**, 17 (2014).
- [5] O. Gomonay, V. Baltz, A. Brataas, and Y. Tserkovnyak, *Nature Physics* **14**, 213 (2018).
- [6] P. Němec, M. Fiebig, T. Kampfrath, and A.V. Kimel, *Nature Physics* **14**, 229 (2018).
- [7] A.V. Kimel, B.A. Ivanov, R.V. Pisarev, P.A. Usachev, A. Kirilyuk, and T. Rasing, *Nature Physics* **5**, 727 (2009).
- [8] A. Kirilyuk, A.V. Kimel, and T. Rasing, *Reviews of Modern Physics* **82**, 2731 (2010).
- [9] P. Wadley, B. Howells, J. Elezny, C. Andrews, V. Hills, R.P. Campion, V. Novak, K. Olejnik, F. Maccherozzi, S.S. Dhesi, S.Y. Martin, T. Wagner, J. Wunderlich, F. Freimuth, Y. Mokrousov, J. Kune, J.S. Chauhan, M.J. Grzybowski, A.W. Rushforth, K.W. Edmonds, B.L. Gallagher, and T. Jungwirth, *Science* **351**, 587 (2016).
- [10] K. Olejník, T. Seifert, Z. Kašpar, V. Novák, P. Wadley, R.P. Campion, M. Baumgartner, P. Gambardella, P. Němec, J. Wunderlich, J. Sinova, P. Kužel, M. Müller, T. Kampfrath, and T. Jungwirth, *Science Advances* **4**, 3566 (2018).
- [11] V. Saidl, P. Němec, P. Wadley, V. Hills, R.P. Campion, V. Novák, K.W. Edmonds, F. Maccherozzi, S.S. Dhesi, B.L. Gallagher, F. Trojánek, J. Kuneš, J. Železný, P. Malý, and T. Jungwirth, *Nature Photonics* **11**, 91 (2017).
- [12] L. Nádvorník, P. Němec, T. Janda, K. Olejník, V. Novák, V. Skoromets, H. Němec, P. Kužel, F. Trojánek, T. Jungwirth, and J. Wunderlich, *Scientific Reports* **6**, 22901 (2016).
- [13] J. Wang, Ł. Cywiński, C. Sun, J. Kono, H. Munekata, and L.J. Sham, *Physical Review B* **77**, 235308 (2008).
- [14] P. Horodyská, P. Němec, T. Novotný, F. Trojánek, and P. Malý, *Journal of Applied Physics* **116**, 053913 (2014).
- [15] P. Wadley, V. Novák, R. Campion, C. Rinaldi, X. Martí, H. Reichlová, J. Železný, J. Gazquez, M. Roldan, M. Varela, D. Khalyavin, S. Langridge, D. Kriegner, F. Máca, J. Mašek, R. Bertacco, V. Holý, A. Rushforth, K. Edmonds, B. Gallagher, C. Foxon, J. Wunderlich, and T. Jungwirth, *Nature Communications* **4**, 2322 (2013).
- [16] P. Wadley, V. Hills, M.R. Shahedkhah, K.W. Edmonds, R.P. Campion, V. Novák, B. Ouladdiaf, D. Khalyavin, S. Langridge, V. Saidl, P. Nemece, A.W. Rushforth, B.L. Gallagher, S.S. Dhesi, F. Maccherozzi, J. Železný, and T. Jungwirth, *Scientific Reports* **5**, 17079 (2015).
- [17] M.J. Grzybowski, P. Wadley, K.W. Edmonds, R. Beardsley, V. Hills, R.P. Campion, B.L. Gallagher, J.S. Chauhan, V. Novak, T. Jungwirth, F. Maccherozzi, and S.S. Dhesi, *Physical Review Letters* **118**, 057701 (2017).
- [18] P. Wadley, S. Reimers, M.J. Grzybowski, C. Andrews, M. Wang, J.S. Chauhan, B.L. Gallagher, R.P. Campion, K.W. Edmonds, S.S. Dhesi, F. Maccherozzi, V. Novak, J. Wunderlich, and T. Jungwirth, *Nature Nanotechnology* **13**, 362 (2018).
- [19] H.-C. Mertins, P.M. Oppeneer, J. Kuneš, A. Gaupp, D. Abramssohn, and F. Schäfers,

Physical Review Letters **87**, 047401 (2001).

[20] N. Tesařová, T. Ostatnický, V. Novák, K. Olejník, J. Šubrt, H. Reichlová, C.T. Ellis, A. Mukherjee, J. Lee, G.M. Sipahi, J. Sinova, J. Hamrle, T. Jungwirth, P. Němec, J. Černe, and K. Výborný, Physical Review B **89**, 085203 (2014).

[21] A.K. Zvezdin and V.A. Kotov, Modern Magneto-optics and Magneto-optical Materials (Taylor & Francis, New York, 2014).

[22] J. McCord, Journal of Physics D: Applied Physics **48**, 333001 (2015).

[23] E. Beaurepaire, J.-C. Merle, A. Daunois, and J.-Y. Bigot, Physical Review Letters **76**, 4250 (1996).

[24] J.-Y. Bigot, M. Vomir, and E. Beaurepaire, Nature Physics **5**, 515 (2009).

[25] V. Saidl, P. Němec, P. Wadley, K.W. Edmonds, R.P. Campion, V. Novák, B.L. Gallagher, F. Trojánek, and T. Jungwirth, Physica Status Solidi (RRL) - Rapid Research Letters **11**, 1600441 (2017).

[26] Z. Kašpar, M. Surýnek, J. Zubáč, F. Křížek, V. Novák, R. P. Campion, M. S. Wörnle, P. Gambardella, X. Marti, P. Němec, K. W. Edmonds, S. Reimers, O. J. Amin, F. Maccherozzi, S. S. Dhesi, P. Wadley, J. Wunderlich, K. Olejník, and T. Jungwirth, *arXiv:1909.09071* (2019).

[27] C.-K. Sun, F. Vallée, L.H. Acioli, E.P. Ippen, and J.G. Fujimoto, Physical Review B **50**, 15337 (1994).

[28] M. Djordjevic, M. Lüttich, P. Moschkau, P. Guderian, T. Kampfrath, R.G. Ulbrich, M. Münzenberg, W. Felsch, and J.S. Moodera, Physica Status Solidi (c) **3**, 1347 (2006).

[29] E. Carpene, E. Mancini, C. Dallera, M. Brenna, E. Puppini, and S.D. Silvestri, Physical Review B **78**, 174422 (2008).

[30] M.H. Kryder, E.C. Gage, T.W. McDaniel, W.A. Challener, R.E. Rottmayer, G. Ju, Y.T. Hsia, and M.F. Erden, Proceedings of the IEEE **96**, 1810 (2008).